Chiang Mai J. Sci. 2016; 43(2) : 276-281
http://epg.science.cmu.ac.th/ejournal/
Contributed Paper

Characterization of NiO-α-MoO_3 Composites Synthesized by Microwave Plasma

Surin Promnopas[a], Orawan Wiranwetchayan [a], Titipun Thongtem [b, c], Wonchai Promnopas*[a] and Somchai Thongtem*[a]

[a] Department of Physics and Materials Science, Faculty of Science, Chiang Mai University, Chiang Mai 50200, Thailand.

[b] Department of Chemistry, Faculty of Science, Chiang Mai University, Chiang Mai 50200, Thailand.

[c] Materials Science Research Center, Faculty of Science, Chiang Mai University, Chiang Mai 50200, Thailand.

*Author for correspondence; e-mail: wonchaicmu@gmail.com, schthongtem@yahoo.com

Received: 15 September 2015
Accepted: 25 November 2015

ABSTRACT

Pure orthorhombic MoO_3 and NiO-MoO_3 composites were successfully synthesized by solid state microwave plasma processing of $(NH_4)_6Mo_7O_{24}\cdot 4H_2O$ and $Ni(NO_3)_2\cdot 6H_2O$ in Ar atmosphere with 3.7 ± 0.1 kPa absolute pressure for 60 min. Phase, morphology, vibration modes and optical properties were characterized by X-ray diffraction (XRD), scanning electron microscopy (SEM), Raman and Fourier transform infrared (FTIR) spectroscopy, and UV-VIS and photoluminescence (PL) spectroscopy. In this research, formation mechanism of the products was also proposed according to the experimental results.

Keywords: NiO-MoO_3 composites, microwave plasma, x-ray diffraction, spectroscopy

1. INTRODUCTION

Recently, there has been extremely interested in improving air quality and global environment. The high level of pollution has driven increasing research and development on a number of semiconducting materials. Molybdenum oxide (MoO_3) and nickel oxide (NiO) are attractive candidates for using as gas detectors, photochromic materials [1-4], and others. α-MoO_3 is a stable n-type orthorhombic phase, has a wide energy gap and is very attractive for different technological applications: smart windows [5], conductive gas sensors [6], lubricants [7] and catalysts [8]. Nickel oxide (NiO) is a p-type semiconductor with 3.6-4.0 eV energy gap at room temperature [9-11] and has a wide range of applications: transparent conductive films, optoelectronic devices [11], electrocatalysts [10] and smart windows [12]. In this research, semiconducting films of α-MoO_3 loaded with 3 wt%, 5 wt% and 10 wt% cubic NiO were synthesized by a clean and fast solid state microwave plasma process [13, 14]. Their energy gaps and emission wavelengths were determined for different technological applications.

2. MATERIALS AND METHODS

2.1 Synthesis

Ammonium molybdate tetrahydrate ($(NH_4)_6Mo_7O_{24}\cdot 4H_2O$) as molybdenum source and nickel (II) nitrate hexahydrate ($Ni(NO_3)_2\cdot 6H_2O$) as nickel source were used without further purification. To synthesize pure α-MoO_3 and NiO-α-MoO_3 composites, each of precursor mixtures of 1.0 g $(NH_4)_6Mo_7O_{24}\cdot 4H_2O$ and 0, 3, 5 and 10 wt% $Ni(NO_3)_2\cdot 6H_2O$ was loaded into a 11 mm I.D.×100 mm long silica tube. Each silica tube was placed in a horizontal (H) quartz tube, which was tightly closed and evacuated to 3.7 ± 0.1 kPa absolute pressure for removal of air. Subsequently, Ar was gradually fed into the H tube. The procedure was repeated three times. Finally, Ar in the H tube was evacuated to 3.7 ± 0.1 kPa absolute pressure. Subsequently, each solid mixture was heated by a 900 W microwave plasma for 5 min, and left cool down in the vacuum to room temperature. The solid was milled and thoroughly mixed for 5 min. Microwave heating was repeated under the same condition until completion of 60 min.

2.2 Characterization

The as-synthesized products were characterized by XRD (Rigaku MiniFlex™ II) operating at 20 kV and 15 mA using Cu K_α line in combination with the JCPDS database [15], SEM (JEOL JSM-6335F) operating at 15 kV, FTIR (Bruker Tensor 27) operating in the range of 400-2000 cm^{-1}, Raman spectrophotometry (T64000 HORIBA Jobin Yvon) using a 50 mW and 514.5 nm wavelength Ar green laser, UV-visible spectrometry (PerkinElmer Lambda 25) and PL spectrometry (PerkinElmer LS 50B) using a 255 nm excitation wavelength at room temperature.

3. RESULTS AND DISCUSSION

3.1 XRD

The effect of NiO content on MoO_3 phase was investigated by XRD (Figure 1). XRD pattern of pure MoO_3 shows five strong intensity peaks at 2q = 23.33, 25.70°, 27.34°, 33.13° and 38.58° which were indexed to the (110), (040), (021), (111) and (060) crystallographic planes of pure orthorhombic MoO_3 (JCPDS database no. 05-0508) with Pbnm space group and space group number of 62 [15]. By doping with 3 wt%, 5 wt% and 10 wt% pure NiO, additional dopant patterns were detected at 2q = 37.28°, 43.30° and 62.91° which were indexed to the (111), (200) and (220) crystallographic planes of cubic NiO (JCPDS database no. 04-0835) [15], respectively. Their intensities gradually increased with the NiO content increase from 3 wt% to 10 wt%. These findings revealed the presence of NiO-MoO_3 composites. Based on orthorhombic MoO_3, its lattice parameters were calculated [13] and were in accordance with those of the JCPDS standard [15]. The average grain size was also determined using the diffraction peaks of MoO_3 and the Scherrer formula [4], and the calculated average grain size was 10.291 nm.

A proposed formation mechanism of MoO_3 and NiO synthesized by microwave plasma is as follows.

$$(NH_4)_6Mo_7O_{24}\cdot 4H_2O(s) \rightarrow 7MoO_3(s) + 6NH_3(g) + 7H_2O(g)$$

$$Ni(NO_3)_2\cdot 6H_2O(s) \rightarrow NiO(s) + 2HNO_3(g) + 5H_2O(g)$$

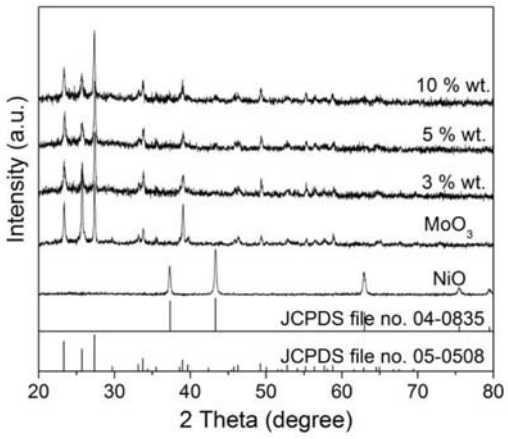

Figure 1. XRD patterns of pure MoO_3, pure NiO, and 3 wt%, 5 wt% and 10 wt% NiO-MoO_3 composites, comparing with their JCPDS nos. 05-0508 (α-MoO_3) and 04-0835 (cubic NiO).

3.2 FTIR and Raman Analyses

FTIR spectra of MoO_3, NiO and NiO-MoO_3 composites are shown in Figure 2(a). Three strong bands were detected at 620, 872 and 993 cm^{-1}, respectively associated with the stretching vibration of oxygen linked with three metal atoms, the stretching vibration of oxygen in the Mo-O-Mo units, and the Mo=O stretching vibration of layered orthorhombic α-MoO_3 phase, very close to the report of Zakharova et al [16]. The broad absorption bands over the 400-500 cm^{-1} range were indexed to the Mo/Ni-O stretching vibration.

Raman spectra of MoO_3, NiO and NiO-MoO_3 composites are shown in Figure 2(b). The 988 cm^{-1} peak was specified as the Mo=O asymmetric stretching vibration of terminal unshared oxygen. The strongest peak at 814 cm^{-1} was specified as doubly coordinated oxygen of Mo_2-O stretching vibration, caused by corner-shared oxygen atoms in common to two MoO_6 octahedrons. The 664 cm^{-1} peak is the Mo_3-O stretching vibration of triply coordinated bridge-oxygen, caused by edge-shared oxygen atoms in common to three octahedrons. These results are in accordance with the report of Klinbumrung et al [13]. These Raman peaks were considered as the fingerprint of α-MoO_3 phase. The pure MoO_3 processed by microwave plasma was highly ordered crystal and its Raman peaks were the highest. The height was reduced in sequence by increasing NiO content from 3 wt% to 10 wt%.

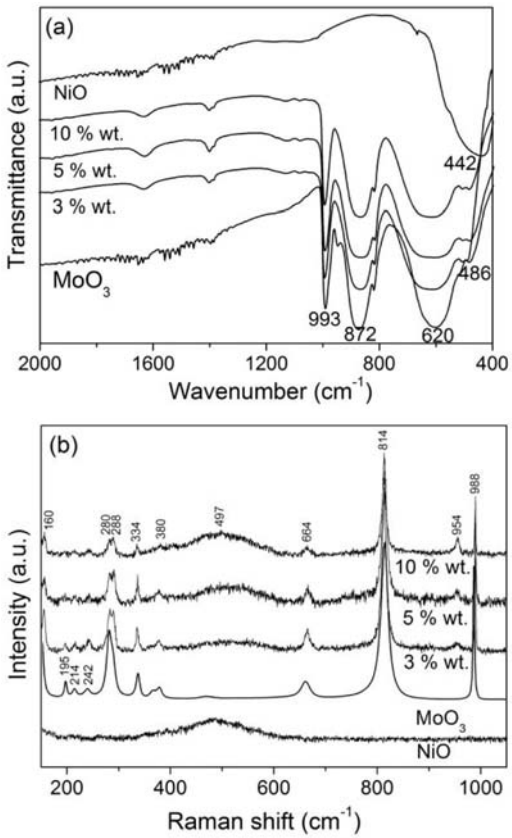

Figure 2. (a) FTIR and (b) Raman spectra of pure MoO_3, pure NiO, and 3 wt%, 5 wt% and 10 wt% NiO-MoO_3 composites.

3.3 SEM

Surface morphologies of NiO, and 3 wt%, 5 wt% and 10 wt% NiO-MoO_3 composites were studied by SEM. Figure 3(a) shows NiO nanoparticles with particle size of approximately 50 nm diameter. The 3 wt%, 5 wt% and 10 wt% NiO-MoO_3 composites (Figure 3b-d) were composed of irregular plates with the size of 50-500 nm.

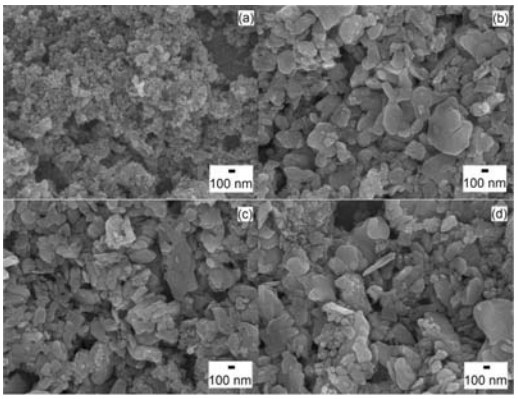

Figure 3. SEM images of (a) NiO, and (b) 3 wt%, (c) 5 wt% and (d) 10 wt% NiO-MoO_3 composites.

3.4 Emission and Absorption

Generally, photonic emission and absorption are the parameters used to evaluate the composites' properties. Thus PL spectra of pure MoO_3, pure NiO, and 3 wt%, 5 wt% and 10 wt% NiO-MoO_3 composites were studied. The spectra (Figure 4) present broad peaks of strong emission centered at 413 nm (violet) and 478 nm (blue), in accordance with the report of Boukhachem et al [17], due to the band-to-band diffusion. Very weak shoulder, caused by electron-hole recombination of the CB and the sublevel of adsorbed oxygen acceptors, was also detected. The shoulder is able to be reduced by high temperature calcination. When the NiO dopant was increased from 3 wt% to 10 wt%, the violet emission became strengthened. For pure NiO, two peaks were detected at 410 nm and 475 nm.

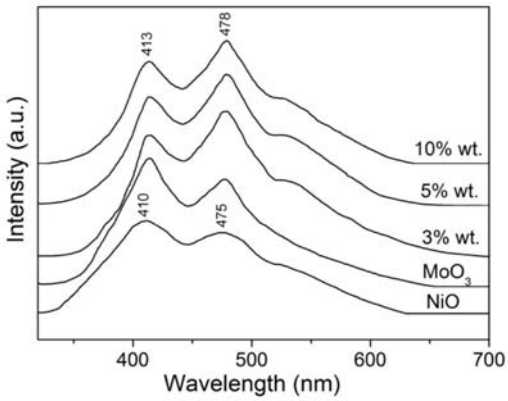

Figure 4. PL emission of pure MoO_3, pure NiO, and 3 wt%, 5 wt% and 10 wt% NiO-MoO_3 composites.

The UV-VIS absorption and the $(\alpha h\nu)^2$ vs $h\nu$ plot of pure MoO_3, pure NiO, and 3 wt%, 5 wt% and 10 wt% NiO-MoO_3 composites are shown in Figure 5. When photon energy is greater than energy gap, the absorption is linearly increased with the increasing of photon energy. Inclination of the linear portion was controlled by charged diffusion from CB to VB. The energy difference is specified as energy gap (E_g). By increasing the NiO content, their energy gap was red shift. By extrapolating the linear portion curve of the $(\alpha h\nu)^2$ vs $h\nu$ plot to zero absorption [9, 11, 18], the direct energy gap was determined to be 4.8-4.9 eV, in accordance with the report of Zhang [11]. In this research, the calculated E_g(NiO) was 3.2 eV.

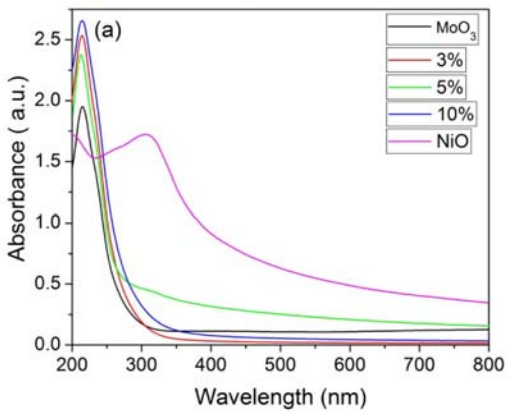

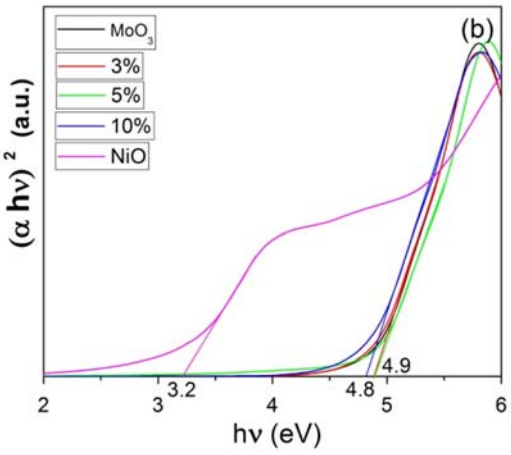

Figure 5. (a) Absorbance and (b) the $(\alpha h\nu)^2$ vs $h\nu$ plot of pure MoO_3, pure NiO, and 3 wt%, 5 wt% and 10 wt% NiO-MoO_3 composites.

4. Conclusions

Pure MoO_3, pure NiO, and 3 wt%, 5 wt% and 10 wt% NiO-MoO_3 composites were synthesized by a 900 W microwave plasma for 60 min. The products were composed of orthorhombic MoO_3 and cubic NiO. The main FTIR and Raman vibration modes were detected at 872 cm^{-1} and 814 cm^{-1}, respectively. Their PL emissions were detected at 413 nm and 478 nm, and their calculated energy gaps were 4.8-4.9 eV.

Acknowledgements

We wish to thank the Thailand's Office of the Higher Education Commission for providing financial support through the National Research University (NRU) Project, Thailand Research Fund (TRF) through the contact IRG5780013, and Graduate School of Chiang Mai University (CMU) through a general support.

References

[1] Alsaifa M.M.Y.A., Balendran S., Field M.R., Latham K., Wlodarski W., Ou J.Z., Kalantar-zadeh K., *Sensor Actuat.*, B 2014; **192**: 196-204.

[2] MalekAlaie M., Jahangiri M., Rashidi A.M., HaghighiAsl A., Izadi N., *Mater. Sci. Semicon. Proc.*, 2015; **38**: 93-100.

[3] Li C., Feng C., Qu F., Liu J., Zhu L., Lin Y., Wang Y., Li F., Zhou J., Ruan S., *Sensor Actuat.*, B 2015; **207**: 90-96.

[4] Shen Y., Yang Y., Hu F., Xiao Y., Yan P., Li Z., *Mater. Sci. Semicon. Proc.*, 2015; **29**: 250-255.

[5] Baetens R., Jelle B.P., Gustavsen A., *Solar Energ. Mater. Solar Cells.,* 2010; **94**: 87-105.

[6] Prasad A.K., Gouma P.I., *J. Mater. Sci.* 2003; **38**: 4347-4352.

[7] Menezes P.L., Ingole S.P., Nosonovsky M., Kailas S.V., Lovell M.R., Tribology for Scientists and Engineers, Springer Science + Business Media N.Y. 2013.

[8] Liu Z., Su H., Li J., Li Y., *Catal. Commun.,* 2015; **65**: 51-54.

[9] Ksapabutr B., Nimnuan P., Panapoy M., *Mater. Lett.*, 2015; **153**: 24-28.

[10] Shibli S.M.A., Harikrishnan G.J., Anupama V.R., Chinchu K.S., Meena B.N., *Surf. Coat. Tech.*, 2015; **262**: 48-55.

[11] Zhang Y., *Appl. Surf. Sci.*, 2015; **344**: 33-37.

[12] Bodurov G., Stefchev P., Ivanova T., Gesheva K., *Mater. Lett.*, 2014; **117**: 270-272.

[13] Klinbumrung A., Thongtem T., Thongtem S., *J. Nanomater.*, 2012; 2012: Art. ID 930763 (5 pp).

[14] Sitthichai S., Thongtem T., Thongtem S., Suriwong T., *Superlatt. Microst.*, 2013; **64**: 433-438.

[15] Powder Diffract. File, JCPDS-ICDD, 12 Campus Bld., Newtown Square, PA 19073-3273, U.S.A., 2001.

[16] Zakharova G.S., Täschner C., Volkov V.L., Hellmann I., Klingeler R., Leonhardt A., Büchner B., *Solid State Sci.*, 2007; **9**: 1028-1032.

[17] Boukhachem A., Kamoun O., Mrabet C., Mannai C., Zouaghi N., Yumak A., Boubaker K., Amlouk M., *Mater. Res. Bull.*, 2015; **72**: 252–263.

[18] Bai S., Chen C., Zhang D., Luo R., Li D., Chen A., Liu C.C., *Sensor Actuat.*, B 2014; **204**: 754-762.